Paper No.
11330

NACE INTERNATIONAL CORROSION 2011 CONFERENCE & EXPO

WATER/HYDROCARBON CO-CONDENSATION AND THE INFLUENCE ON TOP-OF-THE-LINE CORROSION

Thunyaluk Pojtanabuntoeng[1], Marc Singer, Srdjan Nesic
Institute for Corrosion and Multiphase Technology
Ohio University
342 West State Street
Athens, OH 45701

ABSTRACT

Top of the line corrosion (TLC) is a great concern in wet gas transportation where temperature gradient between the internals of the pipeline and the outside environment leads to the condensation of water vapor and a lighter fraction of hydrocarbons. Liquid water from the condensation is greatly corrosive as it is saturated with the acid gases; e.g. CO_2, H_2S, HAc, etc. Extensive work has been previously focused primarily on the hydrocarbon-free systems. In reality, the presence of condensable hydrocarbons affects the overall condensation process as two immiscible liquids with different wettability will form on the steel surface. As a result, less corrosion would be expected if hydrocarbons condense on the steel surface together with water. This work investigates the influence of hydrocarbon co-condensation (n-heptane) on top of the line corrosion. The wettability of water and n-heptane on carbon steel (X65) was determined and corrosion tests under co-condensation were conducted. The results show that following condensation water has higher affinity towards carbon steel than n-heptane in all cases. In a hydrocarbon-free system, corrosion rate increased with the water condensation rate whereas the presence of n-heptane provides some degree of protection in the co-condensation scenario. Under the condition tested where the steel temperature was relatively low (less than 30°C), iron carbonate scale was detected in a co-condensation system but not in a pure water system, suggesting different chemistry in the water condensate phase.

KEY WORDS: Top of the line corrosion, Co-condensation, CO_2 corrosion

[1] Corresponding author, E-mail address: tp127807@ohio.edu (T. Pojtanabuntoeng).

INTRODUCTION

In stratified wet gas transportation, lighter hydrocarbons fractions may co-condense along with water vapor. The condensate is then composed of two immiscible liquid phases water and hydrocarbon, having different abilities to wet the steel surface. Corrosive gases dissolve into the condensed water formed on the upper surface of the pipe resulting in Top-of-the-Line Corrosion (TLC). Extensive research has been conducted and key parameters influencing TLC have been investigated (e.g., temperature, pressure of acid gases, total pressure, acetic acid, etc.) [1-4]. However, those earlier studies focused on hydrocarbon-free systems whereas in reality the co-condensation of hydrocarbons is also present. The presence of hydrocarbons can affect TLC either by changing the wetting of the steel surface or by influencing the water chemistry of the system. Since the hydrocarbons act as a non-electrolyte, it is expected that they will generally lower the CO_2 corrosion rate. It has been established [5-8] that crude oil provides protection to the steel if it displaces water from the steel surface at the bottom of the line. The degree of protection varies with the hydrocarbon type and chemical composition, with heavier crudes generally providing better protection. Tang [8] suggested that surface and Interfacial tension of water and crude oil greatly influence the phase wetting transition in two phase flow condition (water/oil). Lower interfacial tension indicated weak interaction between water and hydrocarbon interface. Thus, water phase was easily entrained into small droplets and maintained in the bulk oil phase.

However, the hydrocarbon fraction that co-condenses with water at the top of the line, differs from that at the bottom, and is fairly light – may range from pentane to nonane. It was thought that such light condensate fractions do not give much protection to the steel from CO_2 corrosion [5], [6]. Yet, it should be pointed out that this referred primarily to the bottom of the line corrosion.

Lotz *et al.* (1991)[6] studied the effect of oil types on CO_2 corrosion of UNS G10180 carbon steel. Several crudes and artificial gas condensate (36 wt.% of C_6, 32 wt.% of C_7 and 32 wt.% of C_8) were selected. Corrosion rates were monitored continuously with Electrochemical Impedance Spectroscopy (EIS) during the stepwise changes in % water cut and flow condition (dispersed or stagnant). Dispersed flow of crude oil and water led to a large scatter of the impedance data associated with low corrosion rate. However, the Nyquist plot did not return to the one semi-circle but two semi-circle shapes were observed implying that another layer of crude oil was present on the steel surface. The hydrocarbon layer gradually desorbed with time. The author also proposed that the corrosion rate theoretically depended on the frequency of the water droplets impinging on the steel surface, their contact area and their residence time. In comparison to co-condensation in TLC, the corrosion rate is directly related to the co-condensation rate of hydrocarbons and water. A higher condensation rate of water refers to a high possibility of water being in contact with the steel.

In order to determine the effect of the presence of hydrocarbons on Top-of-the-Line corrosion, the co-condensation mechanism has to be understood. Since the 1940s, many researchers have been studying and developing mathematical models for heat transfer coefficients of the two-phase condensate [9-10]. Kirkbride (1933) [9] firstly published work on the simultaneous condensation of immiscible liquids. The author noticed different condensation patterns as a function of surface tension and condensation rate. Organic liquids usually formed film and covered the condensing surface due to their low surface tension while water or higher surface tension liquids condensed as drops. As condensation rate increased, the droplets of water or high surface tension liquids could coalesce and condense as film on the surface as well. Afterwards, this study was repeated with different pair of immiscible liquids and the results have been confirmed [9-14]. For instance, Reimann and Mitrovic (1999) [14] investigated the patterns of benzene/water co-condensation on the outer surface of a vertical tube as a function of condensation rate. The authors observed two distinct rivulets on the condensing surface at a low co-condensation rate and stated that the broader one was benzene whereas the narrower was water phase. Nevertheless, the presence of water on the surface was overwhelmed by the benzene condensate at very high co-condensation rate (92% mass of benzene).

However, none were related to corrosion applications. The primary objective of those works was to develop a correlation for heat transfer coefficients of condensate mixtures in condensers or distillation columns. Hence, the experiments were mostly performed in vertical or outer surfaces of horizontal pipes to represent heat exchangers. The orientations of the condensing surfaces affect how two liquids co-condense. Various types and patterns of two-phase condensates produced during the condensation can exist and more than one feature may appear in a real situation. Yet, visual observation, rather than quantitative evidence, was reported.

Wettability is a key property to determine the pattern of co-condensation process. It is defined as "the tendency for one liquid to spread on or adhere to a solid surface in the presence of another immiscible fluid" [7]. Contact angle measurement is the simplest yet most effective method to evaluate the wettability of a liquid on any solid surface. The contact angle (θ_c) can range from 0 to 180^o signifying completely water-wetted surfaces to oil-wetted surfaces, respectively. Figure 1 schematically shows the interaction between water-oil-solid surfaces related through the Young-Dupré equation (Eq. 1). As illustrated in the figure, the surface shows hydrophilic property if the contact angle is less than 90^o and vice versa.

$$\gamma_{os} - \gamma_{ws} = \gamma_{ow} \cos\theta_c \qquad \text{Eq. 1}$$

Where $\gamma_{os}, \gamma_{ws}, \gamma_{ow}$ are interfacial energy between hydrocarbon/solid surface, water/solid surface and hydrocarbon/water, respectively

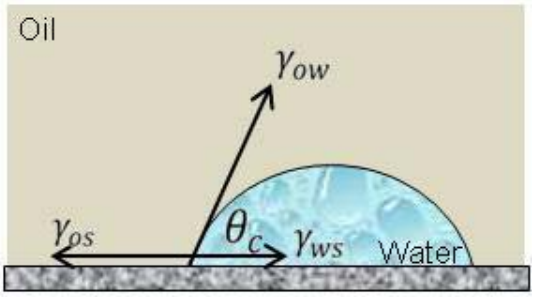

Figure 1: Schematic drawing of water in hydrocarbon contact angle.

Given the poor understanding of corrosion under co-condensation, the main objective of the current research was to investigate the influence of aliphatic hydrocarbons on condensation and TLC.

Condensation rate calculation

Since the current experimental setup does not allow in-situ condensation rate measurement, all the condensation rates are obtained by calculation. A major difference in the condensation of single and binary immiscible components is the heat transfer through the condensate which forms two phase condensate. However, the heat transfer in the vapor phase can be calculated similar to the previous work. [13] The modification was applied to the previous mechanistic model for dropwise condensation for water and Figure 2 illustrates the calculation steps. The total heat flux is the summation of 1.) the latent heat of two condensing liquids (Q_w and Q_{HC}) and 2.) heat flux from the bulk gas to gas-liquid interface (Q_g). The same amount of heat is carried from the gas-liquid interface to the outside environment through several layers of heat resistances. Corresponding temperatures are listed in Figure 3.

Heat transfer from vapor/liquid interface to outside environment was previously considered to be happening through only water droplets. The presence of another immiscible liquid complicates this situation and the heat flux through the hydrocarbon layer is calculated according to laminar film type

condensation[13] [14] and the two heat fluxes (through water and hydrocarbon) are combined by averaging based on volume basis[10].

Figure 4 shows the calculation result. The modification results in slightly lower water condensation rate than the pure water system.

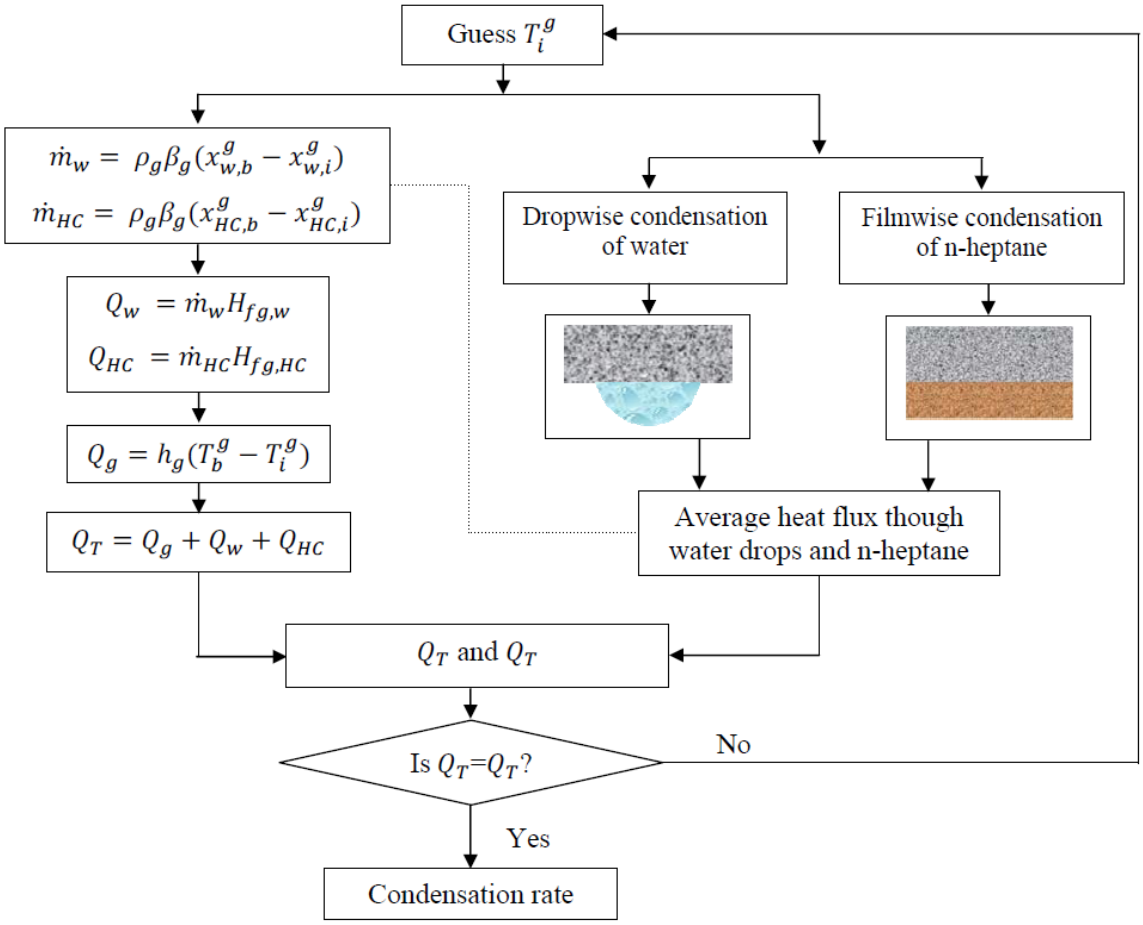

Figure 2: Calculation approach for condensation rate of immiscible liquid: $\dot{m}_w$ is water condensation rate, $\dot{m}_{HC}$ is hydrocarbon condensation rate, ρ_g is gas density, β_g is mass transfer coefficient, $x_{w,b}^g$, $x_{w,i}^g$ are mass fraction of water vapor in bulk gas phase and at the interface, respectively, $x_{HC,b}^g$, $x_{HC,i}^g$ are mass fraction of n-heptane vapor in bulk gas phase and at the interface, respectively, $H_{fg,w}$, $H_{fg,HC}$ are latent heat of vaporization of water and n-heptane vapor, respectively.

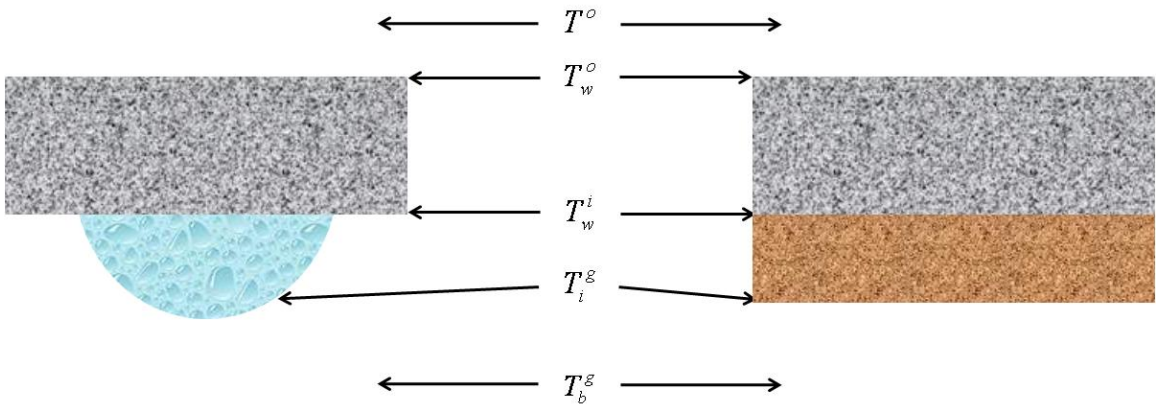

Figure 3: Schematic diagram of the locations of temperatures and two condensation types; Dropwise condensation of water (Left) and Filmwise condensation of n-heptane (Right): T_b^g = Bulk gas temperature, T_i^g = Interfacial gas temperature, T_w^i = Inner pipe wall temperature, T_w^o = outer pipe wall temeprature, T^o = outside temperature

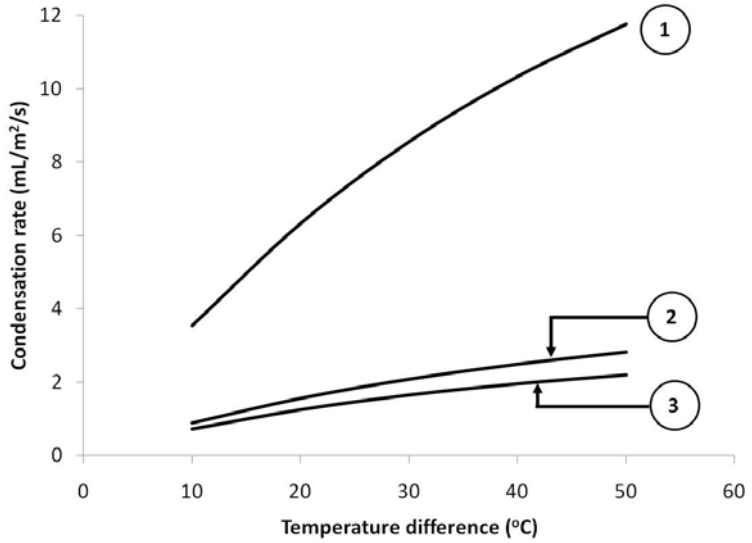

Figure 4: Predicted condensation rates; Line 1 and 3 are water and n-heptane co-condensation rates, respectively and Line 2 is water condensation rates from dropwise calculation. Input conditions are P_T = 3 bar, T_b = 60°C, Pipe Diameter = 0.1 m, Pipe thickness = 15 mm, steel conductivity = 54 W/m/K, and Gas velocity = 5 m/s.

EXPERIMENTAL PROCEDURE

Three sets of tests were conducted including the wettability study, condensation observation, and corrosion tests under different condensation settings. Carbon steel (X65) was used in all tests and n-heptane represented the hydrocarbon phase.

1. Wettability Study

Steel samples were polished with 36 and 600 grit sand paper, rinsed with iso-propanol and air dried. Prior to experiments, surface roughness was determined using a 3D surface profilometry prior to

the experiments. Two roughnesses were prepared as shown in Figure 5. Surface roughness reported in this paper was referred to arithmetic average value (Ra).

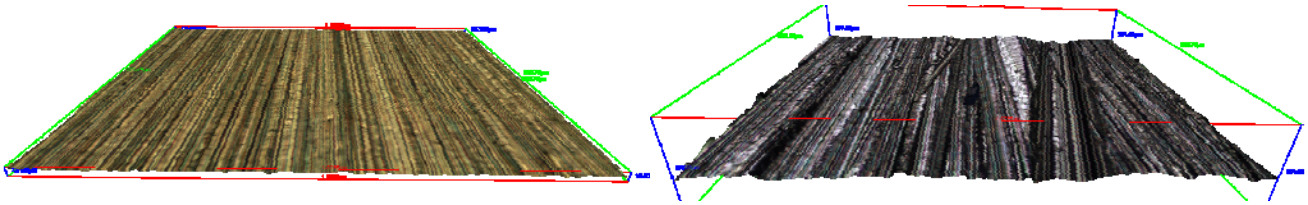

a.) b.)

Figure 5: 3D images of surface prepared at roughness of a.) 0.7 micron and b.) 4 micron.

Contact angles were measured by sessile drop technique in a stainless steel goniometer (Figure 6). Equipment description and procedure were comprehensively explained [17]. Initially, the chamber was filled with DI water saturated with CO_2 at ambient temperature. A carbon steel sample was placed and the system was connected to a digital camera to capture the images. A drop of n-heptane was released in the aqueous phase under the steel surface. Due to its lower density, the drop of n-heptane rose and deposited onto the steel surface, as schematically shown in Figure 6. Three measurements were performed and an arithmetic average value was reported. The experiments were also performed when a water drop was released in an oil continuous phase above the steel surface. Water sunk and deposited on the steel because of its greater density compared to n-heptane.

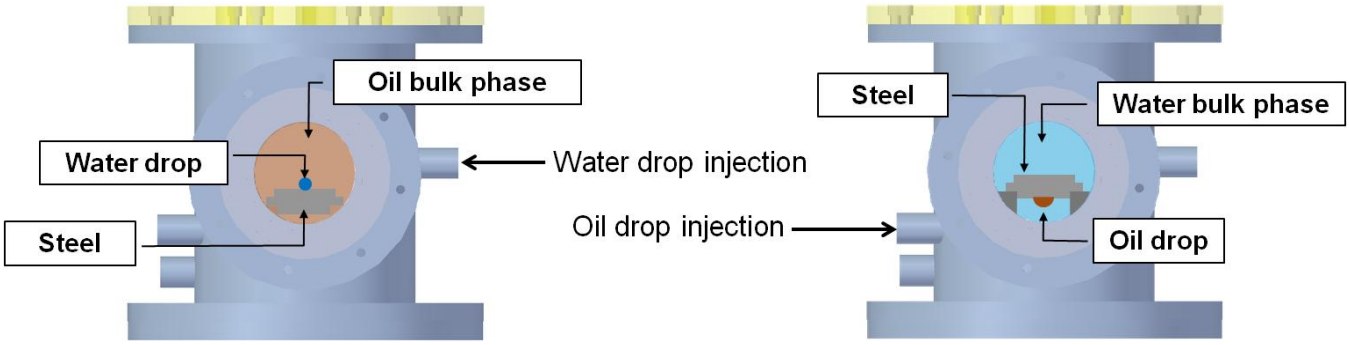

Figure 6: Schematic diagram of goniometer and contact angle measurement procedure [17].

2 Condensation observation

Figure 7 depicts the schematic diagram for the experimental setup used in the visual observation tests. A carbon steel (X65) sample polished with 600 grit sand paper was mounted on the underside of a stainless steel lid and was artificially cooled with a thermoelectric cooler (Peltier). Hot vapor of n-heptane and water were generated by adjusting the liquid phase temperature to achieve the desired vapor temperature. Vapor temperature was range from 30 to 50^{o}C while the sample temperature was between 25 to 40^{o}C. Condensation rates were then calculated using the approach described above. CO_2 was bubbled throughout the experiment in order to acidify the condensed water and to help transport water from underneath to the vapor phase. Vigorous bubbling can create splash droplets altering the condensation process on the sample and, hence it was reduced. Vapor and sample temperature were constantly recorded. A borescope was used to monitor the condensation process.

To study the effect of condensation sequence, a single liquid condensation was firstly performed until reaching the steady state where no change in condensation process was observed. Subsequently, the second liquid was introduced into the cell and the change in condensation process was monitored.

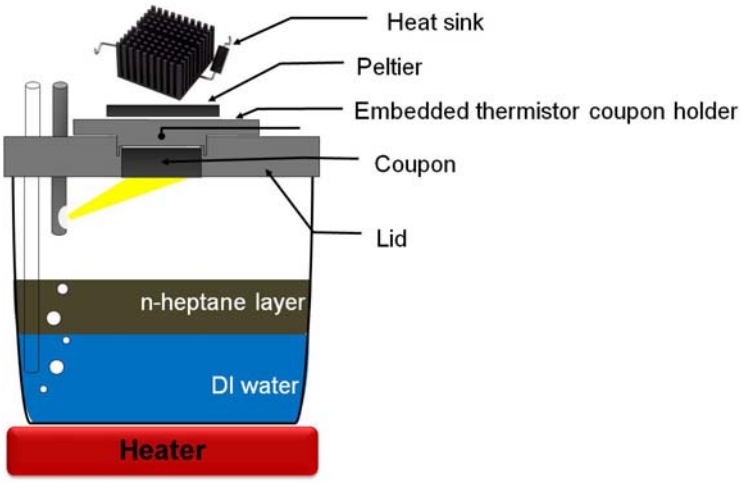

Figure 7: Schematic drawing of setup used for the condensation observation experiments.

Table 1
Compositional analysis of carbon steel (X65)

Element	Al	As	B	C	Ca	Co	Cr	Cu	Mn	Mo	Nb
%Wt.	0.032	0.008	0.001	0.13	0.002	0.007	0.14	0.131	1.16	0.16	0.017
Element	Ni	P	Pb	S	Sb	Si	Sn	Ta	Ti	V	Zr
%Wt.	0.36	0.009	<0.001	0.009	0.009	0.26	0.007	<0.001	<0.001	0.047	<0.001

Table 2
Test Matrix for condensation observation experiments

Parameters	Conditions
Material	X65
Carrier gas	CO_2
Total pressure (bar)	1
Liquids	Water n-heptane A heterogeneous mixture of water and n-heptane
Condensation sequences	Water → n-heptane n-heptane → Water Water + n-heptane

3 Corrosion test by weight loss measurement

A very similar experimental setup as described above was used but without the borescope. The experimental parameters are described in Table 3. The calculated condensation rates of water and n-heptane are given in Table 4. Due to the limitation of this setup, high condensation rate could not be achieved. Water and n-heptane were deoxygenated by purging with CO_2 overnight at ambient temperature. Subsequently, a steel sample was placed onto the lid and cooled while hot vapor was generated. During the test, n-heptane coud be quickly depleted compared to water. A deoxygenated n-heptane was constantly added to avoid the depletion.

Once the experiments were finished, the samples were analyzed with Scanning Electron Microscope (SEM) and Energy-Dispersive X-ray spectroscope (EDX). Clarke's solution was prepared to remove the corrosion product on the surface (20 gms of Sb_2O_3 and 50 gms of $SnCl_2$ in one litre of Concentrated HCl). Weight loss due to corrosion was then calculated. A 3D surface profilometer was used to identify if there is any localized attack. All tests were repeated twice and three times in low co-condensation conditions.

RESULTS

1. Wettability Study

Figure 8 shows images of water in n-heptane contact angle measurements (top and bottom). The contact angle is always measured through the water phase. The smooth coupon with an average surface roughness (R_a) of 0.7 ± 0.2 micron exhibits hydrophilicity quicker than that with the rougher surface as the contact angles were instantaneously below 90^o (Figure 8a). On the rougher surface (R_a = 3.6 ± 0.4 micron), the water drop required longer time to reach hydrophilic region. Vice versa, the contact angles of n-heptane drop in the presence of water were illustrated in Figure 8b. Again, carbon steel surface shows hydrophilic properties as contact angle is less than 90^o. Roughness shows no influence on the contact angle in this case (Figure 8b).

Table 3
Test Matrix for corrosion experiments

Parameters	Conditions
Material	X65
Carrier gas	CO_2
Total pressure (bar)	1
Hydrocarbon representative	n-heptane
Vapor temperature (^{o}C)	35-50
Sample temperature (^{o}C)	25-30
Condensation sequences	Water → n-Heptane n-heptane → Water Water + n-heptane
Test duration (days)	3
Water:Hydrocarbon ratio	According to vapor temperature

Table 4
Calculated condensation rates corresponding to the temperature gradient

Condition	Vapor Temperature (^{o}C)	Sample temperature (^{o}C)	Water condensation (mL/m^2/s)	Co-condensation (mL/m^2/s)	
				WCR	HCCR
Low	35	25	0.023	0.02	0.48
Medium	50	30	0.092	0.07	1.57

***Note**: WCR and HCCR are water condensation rate and n-heptane condensation rate, respectively.

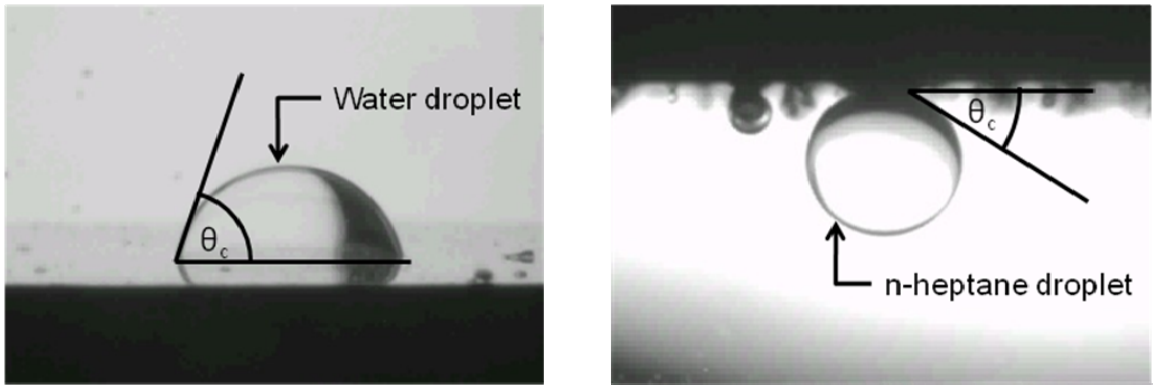

Figure 8: Typical images for contact angle for water in oil (Left) and oil in water (Right).

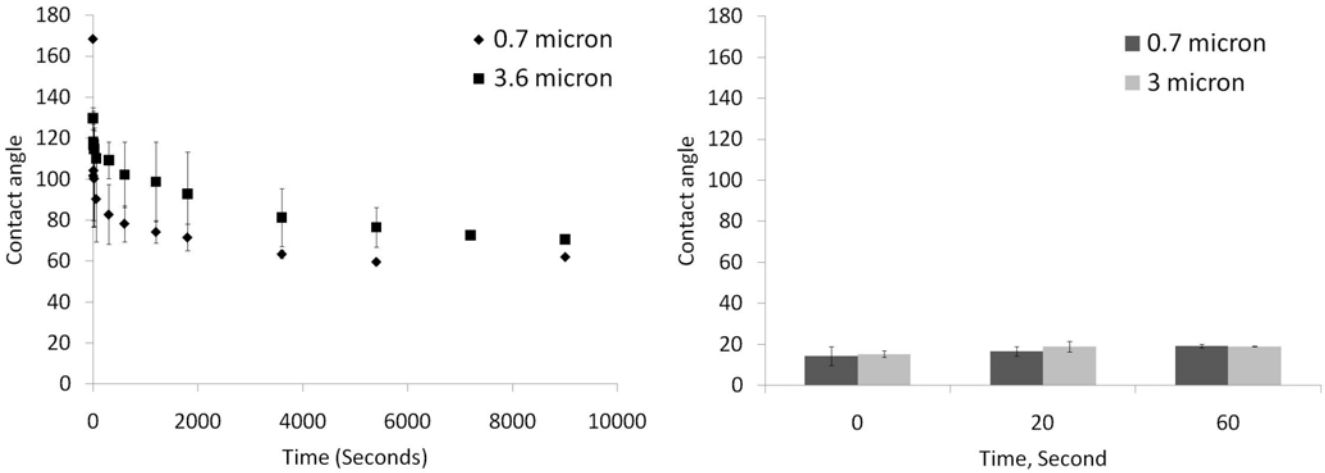

a.) b.)

Figure 9: The contact angles of a.) water in n-heptane and b.) n-heptane in water on two difference roughnesses versus time.

2 Condensation observations

Water, which has a higher surface tension compared to n-heptane, started condensing as isolated droplets (Figure 10a and b). Consequently, adjacent drops coalesced and grew (Figure 10c and d). Once a given droplet reached its maximum size, the gravity force exceeded the surface tension and buoyancy force, the drop fell down. This allowed newly condensed water to occupy the same area (Figure 10e). Higher condensation rate of water was still initiated by forming isolated drops but the coalescence of nearby droplets proceeded more rapidly. The condensation of n-heptane, on the other hand, took place differently as it condensed in a filmwise manner (Figure 11). No distinct droplet of n-heptane was observed. Once the accumulation of n-heptane layer on the surface reached the limit, n-heptane fell down due to gravity.

Though the contact angle showed that carbon steel is hydrophilic and prefers water, water condensation still initiated as droplets while n-heptane spread easily on the carbon steel. This observation posed the question whether the dropwise condensation of water and filmwise condensation of n-heptane on the steel conflict the result wettability results describe earlier? Since contact angle describes the interactions at the water/n-heptane/steel interface, it can be interpreted only in a co-condensation scenario. Therefore, the contact angle measured here does not describe the initiation of the condensation of a single liquid, and there is no contradiction.

Simultaneous condensation was conducted and the co-condensation process is illustrated in Figure 12. n-heptane appeared to condense first, as shown in Figure 12b. Later, the water phase was detected on the surface but no coalescence of those water drops was observed within 3 hours (Figure 12c and d). At the end of the test, those drops were confirmed to be water using cobalt chloride paper (humidity indicator). Though water has a stronger attraction for steel, it could not fully remove the n-heptane and occupy the entire steel area on the sample.

In real transmission pipelines, the gas composition fluctuates with time. Components that condense on the specific area may periodically vary. Thus, the next series of test were done to observe the influence of condensing order. Figure 13a displays the steady state condensation of water prior to adding n-heptane into the system. The condensation of water also happened on the stainless steel lid but different characteristic was observed due to different condensation rate and different surface preparation. The carbon steel sample was artificially cooled leading to higher condensation rate comparing to the lid. In addition, the sample was polished while the lid was not. Liquid has more difficulty to spread onto rougher surface thus showing many droplets of water on the lid area. Figure 13b and c. illustrate that n-heptane started condensing on the sample surface and altered the wetting behavior of water as the water film was interrupted and formed droplets instead. The white spots could be referred to the tips of the small droplets reflecting the light from the camera.

The order of condensation was then reversed. The n-heptane initially condensed on the steel. Water was introduced after steady state of n-heptane condensation was reached. Subsequently, small drops of water started forming on the surface (Figure 14b). As the process continued (Figure 14c), more droplets of water were present but no significant coalescence of water droplets was observed.

a.) 0 minute

b.) 5 minutes

c.) 10 minutes

d.) 20 minutes

e.) 30 minutes

Figure 10: Condensation behavior of water with time (WCR = 0.03 mL/m^2/s).

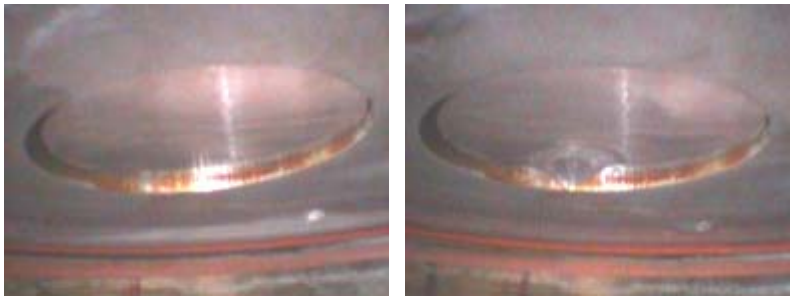

a.) b.)

Figure 11: Condensation process of n-heptane (HCCR = 0.1 mL/m^2/s).

a.) 0 minute b.) 30 minutes c.) 180 minutes

Figure 12: Condensation observation when both phases co-condensed (WCR = 0.017 mL/m^2/s, HCCR = 0.43 mL/m^2/s).

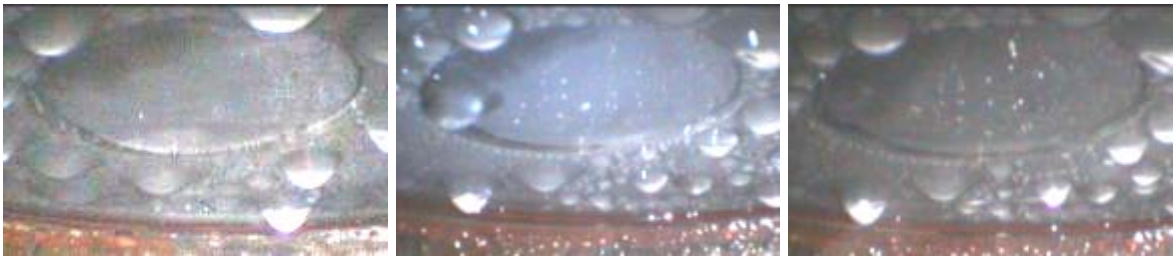

a.) b.) c.)

Figure 13: Condensation observation when water condensed first (WCR = 0.068 mL/m^2/s, HCCR = 1.46 mL/m^2/s).

a.) b.) c.)

Figure 14: Condensation observation when a.) n-heptane firstly condensed, b.) 15 minutes after adding water, and c.) 30 minutes after adding water (WCR = 0.012 mL/m^2/s, HCCR = 0.31 mL/m^2/s)

3 Corrosion test weight loss measurement

In hydrocarbon-free system, the corroded surface was mostly uniform (Figure 15 – Figure 17). No iron carbonate ($FeCO_3$) was detected either with EDX analysis or visual observation under SEM (crystalline particles on the surface). The iron carbonate formation occurs by precipitation process. Thus, the solubility of Fe^{2+} and CO_3^{2-} need to exceed the "solubility limit". Considering the low CO_2 content and the constant renewal of water droplets, the high supersaturation conditions could probably not be achieved. In addition the kinetics of $FeCO_3$ precipitation was slow due to low surface temperature (25^{o}C and 30^{o}C)

Intriguingly, crystalline particles of iron carbonate were observed in all co-condensation environments suggesting different chemistry in water condensate when n-heptane was present (Figure 18 and Figure 19). The possible reason for this finding is that water is "trapped" by n-heptane on the surface. Therefore, the ferrous ions released from the corrosion process have more time to accumulate and exceed the $FeCO_3$ solubility limit. However, the $FeCO_3$ seems to be loosely formed and not cover the entire surface. Therefore, it did not contribute to any protection.

After removing the corrosion product with Clark's solution, both SEM and 3D surface profilometry revealed that n-heptane was present in between the water drops since the polishing marks were still noticed (Figure 20-Figure 23). This is in contrast with water condensation system where the entire surface is uniformly corroded. No severe localized corrosion was found in either system, probably due to insufficient test duration (3 days). Figure 24 shows corrosion rates as a function of condensation rates whereas Table 5 shows tabulated data. Black bars represent corrosion rates obtained from weight loss whereas grey bars indicate the thickness loss from 3D surface profilometry. Error bars specify the minimum and maximum values in the repeated tests. In hydrocarbon-free system (Figure 24a), the corrosion proceeds faster at high water condensation rates. On the other hand, the presence of n-heptane seemed to cause reverse behavior (Figure 24b). The corrosion rate decreased when both liquids condense more. Though there was an increase in water condensation rate (from 0.02 to 0.07 $mL/m^2/s$), this increase was even more pronounced for n-heptane (from 0.48 to 1.57 $mL/m^2/s$). Thus, the interference of n-heptane with water wetting of the steel surface was more pronounced and the corrosion rate was lower.

The presence of n-heptane at low co-condensation rate unexpectedly increased the corrosion rate of carbon steel from 0.17 to 0.55 mm/yr. Three repetitions were done to validate the result. The possible explanation is that the amount of condensed n-heptane is not enough to remove water from being in contact with the steel. Additionally, CO_2 solubility in n-heptane is very high and n-heptane can serve as the reservoir of CO_2

.

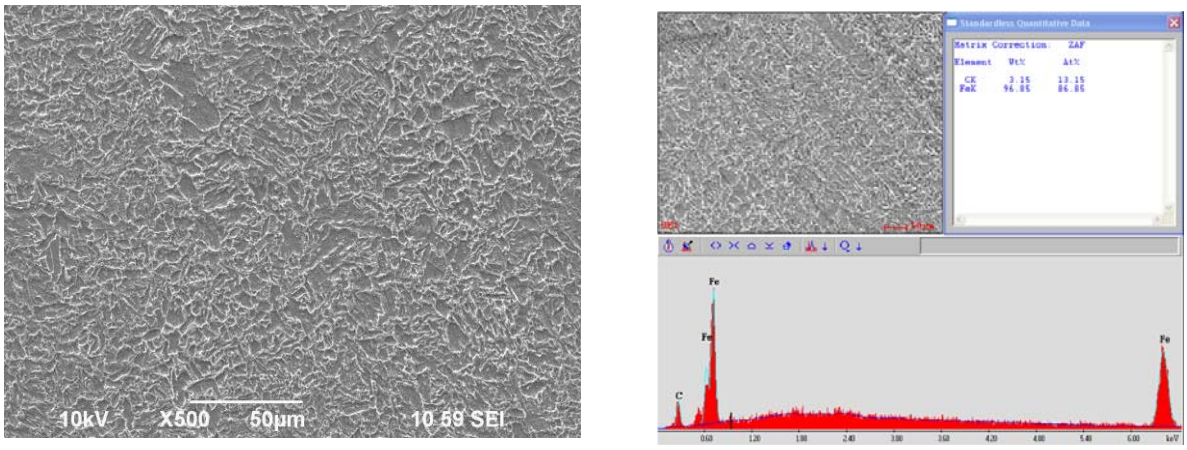

Figure 15: SEM images and EDX analysis of sample exposed to low water condensation (0.02 mL/m^2/s).

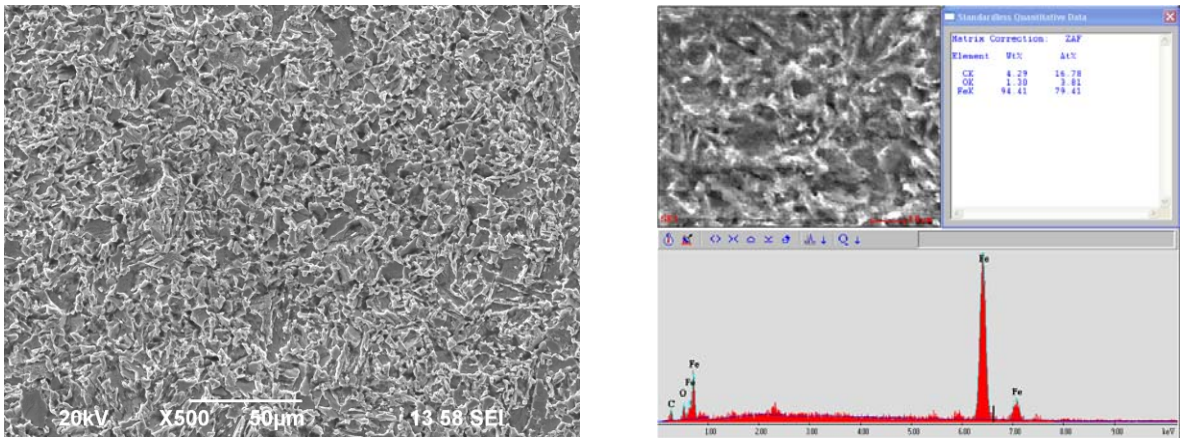

Figure 16: SEM Images and EDX analysis of sample exposed to high water condensation (0.09 mL/m^2/s).

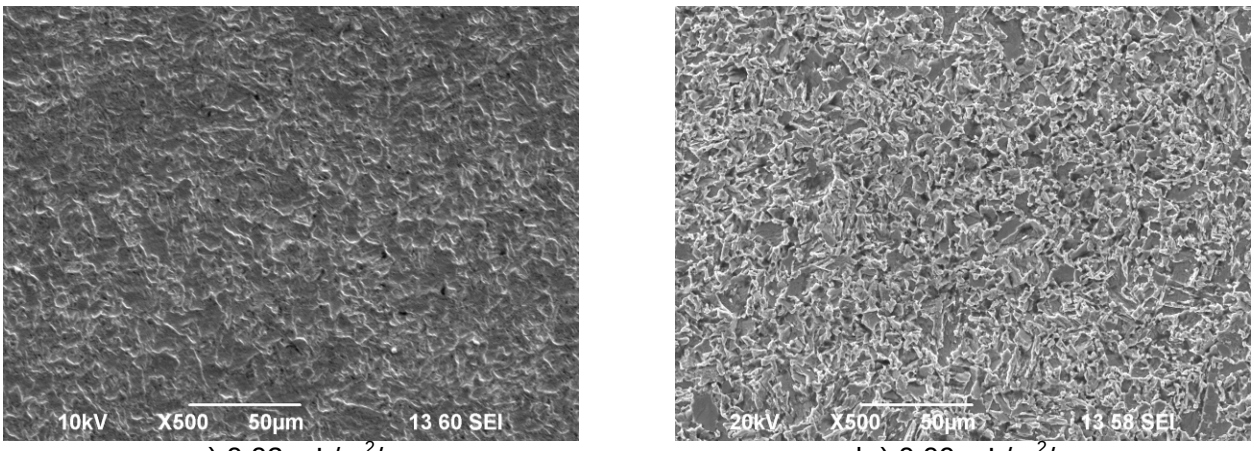

a.) 0.02 mL/m^2/s b.) 0.09 mL/m^2/s

Figure 17: SEM Images of samples exposed to water condensation after cleaning with Clark's solution.

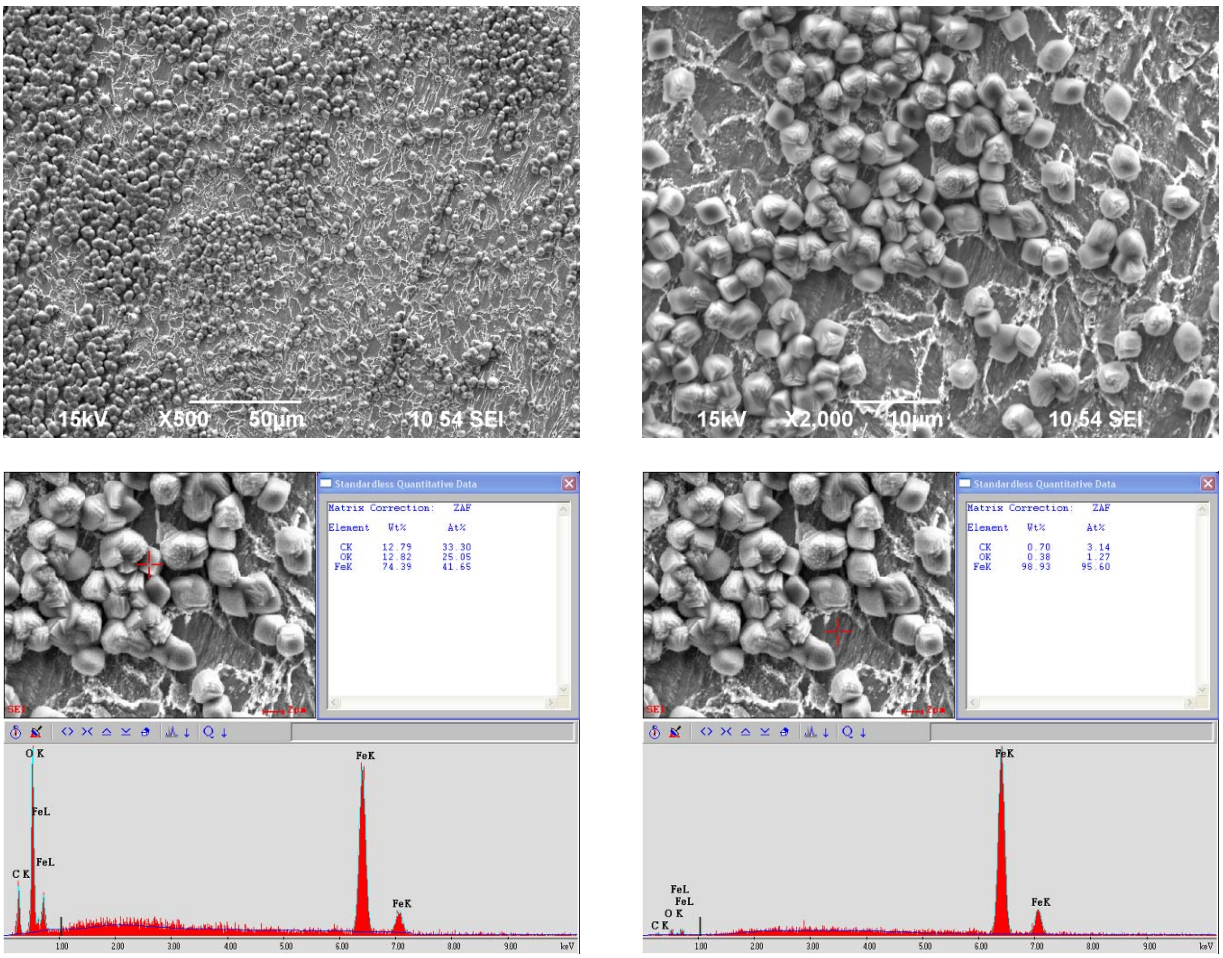

Figure 18: SEM Images and EDX analysis of sample exposed to low co-condensation (WCR and HCCR = 0.02 and 0.48 mL/m2/s, respectively).

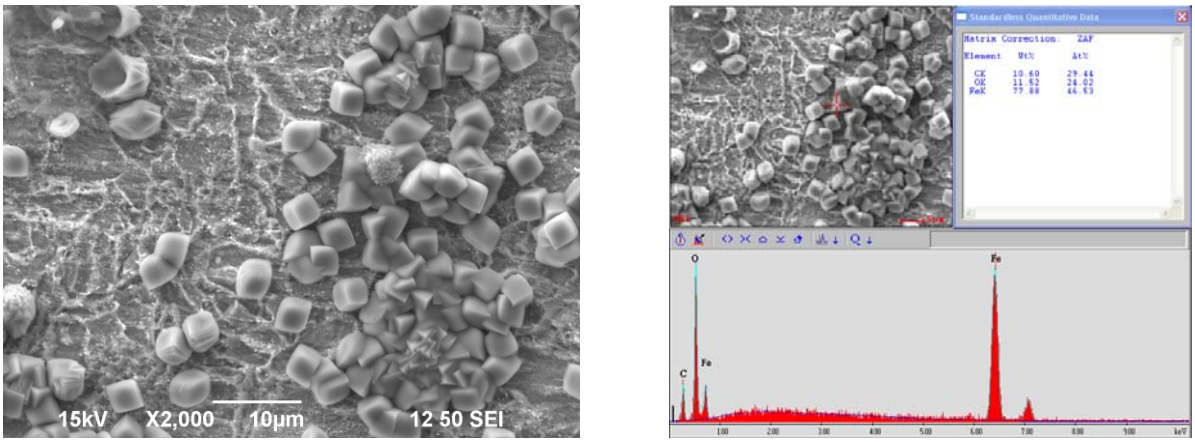

Figure 19: SEM Images and EDX analysis of sample exposed to high co-condensation (WCR and HCCR = 0.07 and 1.57 mL/m^2/s, respectively).

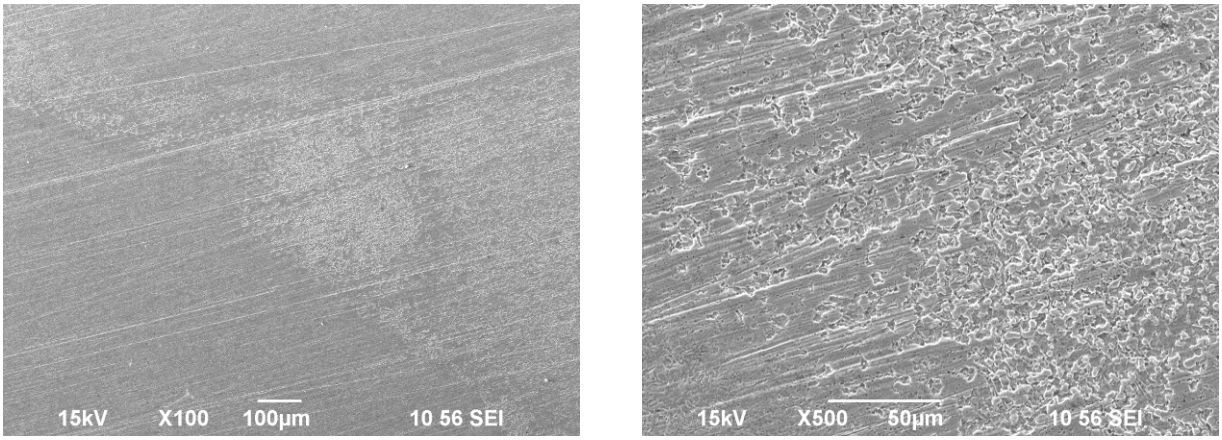

Figure 20: SEM Images of sample exposed to low co-condensation after cleaning with Clark's solution (WCR and HCCR = 0.02 and 0.48 mL/m2/s, respectively).

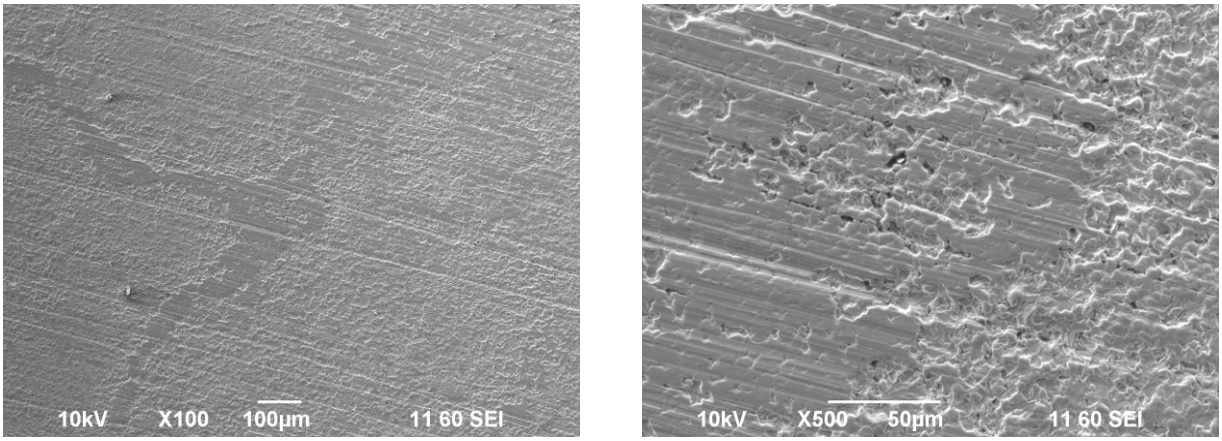

Figure 21: SEM Images of sample exposed to high co-condensation after cleaning with Clark's solution (WCR and HCCR = 0.07 and 1.57 mL/m^2/s, respectively).

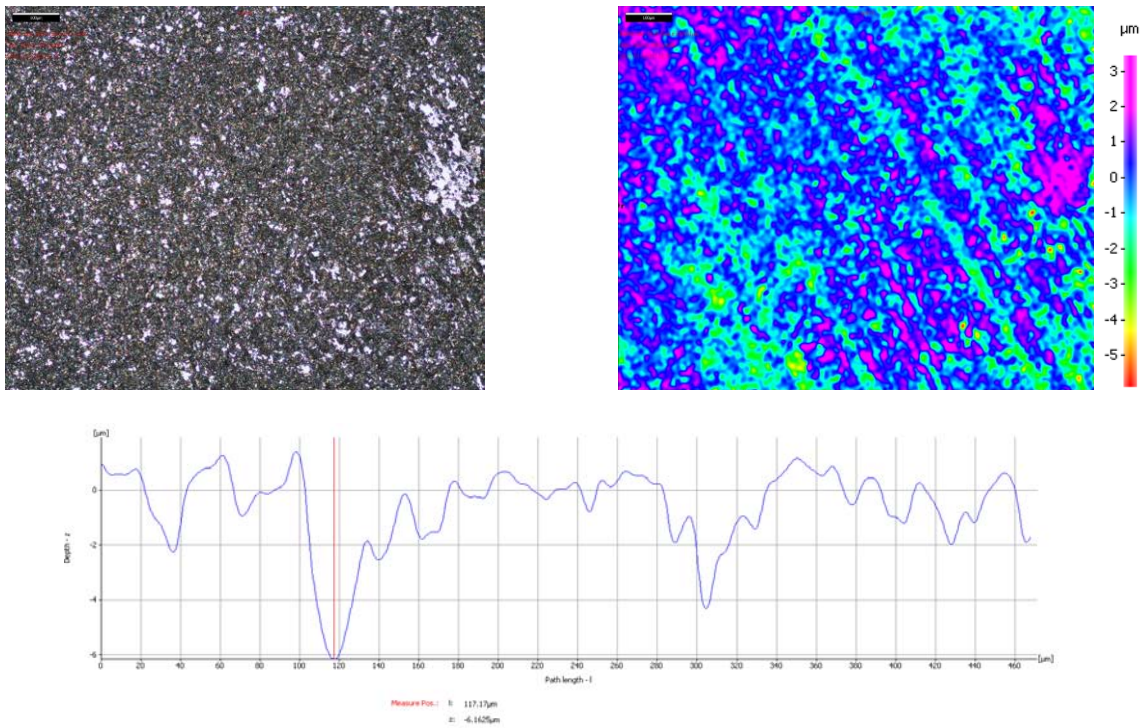

Figure 22: 3D surface profilometry of sample exposed to water condensation rate of 0.09 mL/m^2/s.

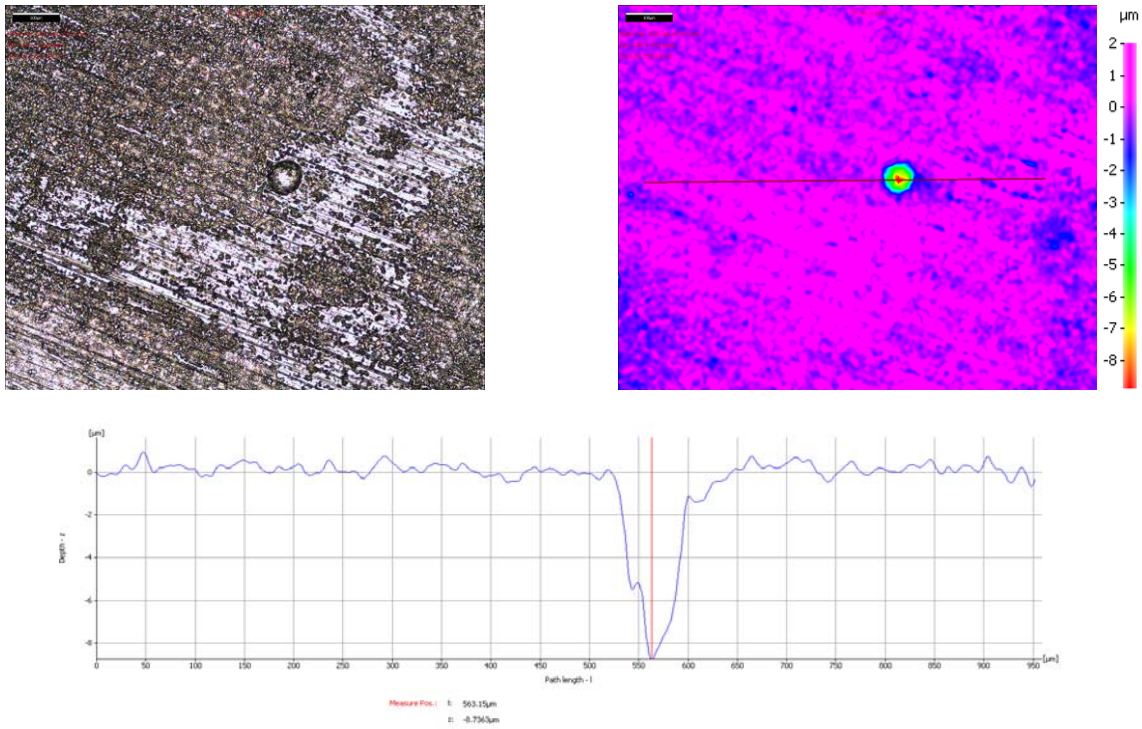

Figure 23: 3D surface profilometry of sample exposed to low co-condensation.

Table 5
Corrosion rates

Condensation rate ($mL/m^2/s$)		Corrosion rate (mm/yr)	
WCR	HCCR	Weight loss	Maximum localized corrosion
0.02	0	0.17	0.30
0.09	0	0.50	0.80
0.02	0.48	0.55	0.89
0.07	1.57	0.13	0.54

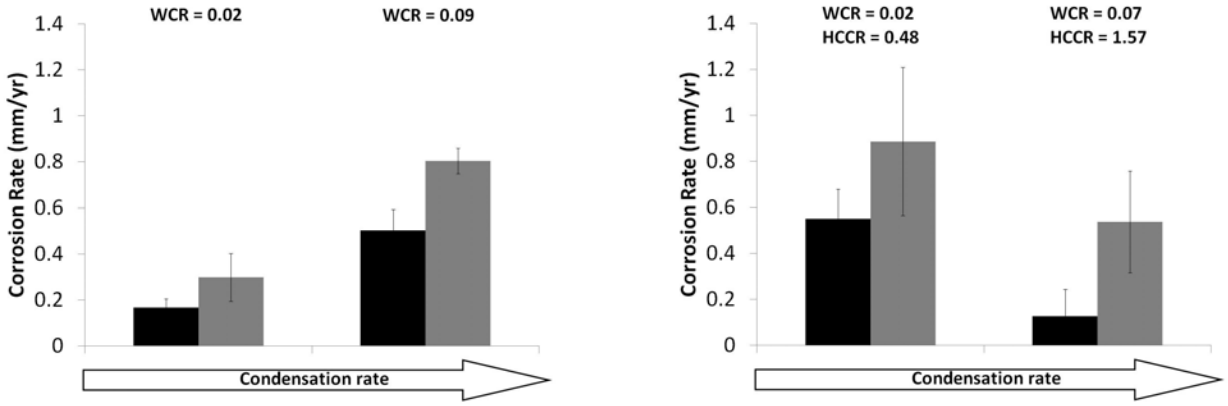

a.) b.)

Figure 24: Corrosion rates with condensation rate in (a) hydrocarbon-free system and (b) co-condensation system

CONCLUSIONS

- The results from the wettability test shows that carbon steel is hydrophilic and it is preferentially wetted with water in a co-condensation scenario. However, as contact angle is still below 180^o, n-heptane can be incontact with the steel surface to some extent.
- In co-condensation scenario, n-heptane is suspected to condense as a film in between droplets of water.
- In the absence of n-heptane, water condensation rate increases the corrosion rates.
- In the presence of n-heptane the corrosion rate decreases with an increase in co-condensation rate.

ACKNOWLEDGEMENTS

The authors would like to acknowledge the technical guidance and financial support provided by the sponsor companies of the Top of the Line Corrosion Joint Industry Project at Ohio University: Total, BP, ConocoPhillips, Chevron, Saudi Aramco, Occidental Oil Company, ENI, and PTTEP.

REFERENCES

[1] Y.M. Gunaltun, D. Larrey, “Correlation of Cases of Top of Line Corrosion with Calculated Water Condensation Rates,” CORROSION/2000, paper no. 071 (Houston, TX: NACE, 2000).

[2] M. Singer, D. Hinkson, Z. Zhang, H. Wang, S. Nesic, "CO_2 Top of the Line Corrosion in Presence of Acetic Acid: A Parametric Study," CORROSION/2009, paper no. 292 (Houston, TX: NACE, 2009).

[3] D. Hinkson, M. Singer, Z. Zhang, S. Nesic "A Study Of The Chemical Composition and Corrosivity of the Condensate for Top of the Line CO_2 Corrosion," CORROSION/2008, paper no. 466 (Houston, TX: NACE, 2008).

[4] C. Mendez, M. Singer, A. Camacho, S. Nesic, S. Hernandez, Y. Sun, Y. Gunaltun, M.W. Joosten, P. Gabbetta, “Effect of Acetic Acid, pH and MEG on the CO2 Top of the Line Corrosion,” CORROSION/2005, paper no. 378 (Houston, TX: NACE, 2005).

[5] C. Waard and U. Lotz, “Prediction of CO_2 Corrosion of Carbon Steel,” CORROSION/1993, paper no. 69 (Houston/TX: NACE, 1993).

[6] U. Lotz, L. van Bodegom, C. Ouwehand, "The Effect of Type of Oil or Gas Condensate on Carbonic Acid Corrosion," *Corrosion* 47, (1991): pp. 635-644.

[7] J.S. Smart, "Wettability - A Major Factor in Oil and Gas System Corrosion," *Materials Performance* 40: (2001), pp. 54-59.

[8] X. Tang, C. Li, F. Ayello, J. Cai, S. Nesic, “Effect of Oil Type on Phase Wetting Transition and Corrosion in Oil-Water Flow,” CORROSION/2007, paper no. 170 (Houston, TX: NACE, 2007).

[9] C. Kirkbride, "Heat Transmission by Condensing Pure and Mixed Substances on Horizontal Tubes," *Industrial & Engineering Chemistry* 25 (1933): pp. 1324–1331.

[10] W. Akers, M. Turner, "Condensation of Vapors of Immiscible Liquids," *AIChE Journal* 8: (1962), pp. 587–589.

[11] S.H. Bernhardt, J.J. Sheriden, J.W. Westwater, "Condensation of Immiscible Mixtures,” *AIChE Journal* 68: (1972), pp. 21-37.

[12] A. Boyes, A. Ponter, "Condensation of Immiscible Binary Systems," *CPE-Heat Transfer Survey* (1972), pp. 26-30.

[13] O. Tutkun, "Condensation of Vapours of Binary Immiscible Liquids," *Chemical Engineering and Processing* 32: (1993), pp. 263-272.

[14] E. Reimann and J. Mitrovic, “Patterns of Condensate Flow and Heat Transfer with Condensation of Vapour Mixtures Forming Immiscible Liquids,” *Heat and Technology* 17, 2 (1999): pp. 71-79.

[15] Z. Zhang, D. Hinkson, M. Singer, H. Wang, S. Nesic, “A Mechanistic Model of Top of the Line Corrosion,” CORROSION/2007, paper no. 556 (Houston, TX: Nace, 2007).

[16] J.M. Martin-Valdepenas, M.A. Jimenez, F. Martin-Fuertes, J.A. Fernandez. Benitez “Comparison of Film Condensation Models in Presence of Non-Condensable Gases Implemented in a CFD Code,” *Heat Mass Transfer* 41: (2005), pp. 961-976.

[17] X. Tang, S. Richter, S. Nesic, “Study of Wettability of Different Mild Steel Surface,” 17th International Corrosion Congress, 2008.